

# Quark-Meson Coupling model based upon the Nambu-Jona Lasinio model

D. L. Whittenbury, M. E. Carrillo-Serrano, A. W. Thomas

*CSSM and ARC Centre of Excellence for Particle Physics at the Terascale,  
School of Physical Sciences, University of Adelaide, Adelaide SA 5005, Australia*

---

## Abstract

The NJL model for the octet baryons, using proper time regularization to simulate some of the features of confinement, is solved self-consistently in nuclear matter. This provides an alternative framework to the MIT bag model which has been used in the quark-meson coupling model. After fitting the parameters of the model to the saturation properties of symmetric nuclear matter the model is used to explore the equation of state of pure neutron matter as well as nuclear matter at densities relevant to heavy ion collisions. With a view to future studies of high mass neutron stars, the binding of hyperons is also explored.

*Keywords:* Hadron structure, Nuclear matter, Equation of state, QMC model, NJL model, Faddeev equation  
*PACS:* 12.39.-x, 21.65.Mn, 14.20.Jn

---

## 1. Introduction

There is little doubt that Quantum Chromodynamics (QCD) is the correct theory of the strong interaction. However, the issue of connecting this more fundamental theory to traditional nuclear physics is extremely challenging. Of course, we have hints of what might be involved through phenomena such as the EMC effect [1, 2] but we are far from a full understanding of the influence of quark degrees of freedom and their implications for the complex phenomena emerging from QCD.

The Quark-Meson Coupling (QMC) model goes beyond the majority of nuclear models by explicitly treating baryons as extended objects. It is a relativistic quark level model which has been extensively used to study nuclear matter [3], finite nuclei [4] and neutron stars [5]. The model has recently been shown to provide a remarkably accurate description of the ground-state properties of atomic nuclei across the periodic table, in terms of a derived, density-dependent effective NN potential [6]. Within QMC the MIT bag model is used as the model of hadron structure, although one need not restrict oneself to this. Indeed, it is clearly of interest to extend the approach to other models of hadron structure. For example, Bentz and Thomas [7] were the first to develop such a theory by hadronising the NJL model, which embodies different aspects of QCD, notably spontaneous chiral symmetry breaking. The aim of this letter is to consider the effect of hadron structure on nuclear matter properties within this complementary model.

Within the QMC model the in-medium changes of the baryon properties, such as masses, scalar cou-

plings and so on, are calculated by self-consistently solving the bag equations, including the effect of the mean fields generated by other nucleons. The masses are then parametrised as functions of the mean scalar field as

$$M_B^* = M_B - w_B g_{\sigma N} \bar{\sigma} + \frac{d}{2} \tilde{w}_B (g_{\sigma N} \bar{\sigma})^2, \quad (1)$$

(where the weightings  $w_{\sigma B}$  and  $\tilde{w}_{\sigma B}$  simply allow us to express the density dependent couplings of the mean scalar field to each hadron in terms of the unique coupling to the nucleon in free space,  $g_{\sigma N}$ . Using this parametrisation and the corresponding density dependent coupling, we can solve for the equation of state in a manner analogous to the Walecka model [8, 9, 10, 11], that is at the hadronic level. In this way the sub-structure of the baryons is entirely contained in the mass parametrisation. In Ref. [12, 13, 14], we used the bag model parametrisation given in Ref. [15], which includes the effects of one gluon exchange. Here we present a new variation of the QMC model with a mass parametrisation obtained by solving the Faddeev equation derived from the proper time regularised NJL model. Then, using this new mass parametrisation, we calculate the equations of state of Symmetric Nuclear Matter (SNM) and Pure Neutron Matter (PNM) in a Hartree-Fock approximation.

In Ref. [13] we extended the QMC model by performing a Hartree-Fock calculation including the full vertex structure for the vector mesons. This extension only alters the exchange contribution, including not only the Dirac vector term, as was done in Ref. [5], but also the Pauli tensor term. These terms were already included within the QMC model by Krein *et*

$m_\ell$ [MeV]	$m_s$ [MeV]	$M_\ell$ [MeV]	$M_s$ [MeV]	$\Lambda_{\text{IR}}$ [MeV]	$\Lambda_{\text{UV}}$ [MeV]	$G_\pi$ [GeV <sup>-2</sup> ]	$Z_\pi$	$Z_\pi(0)$
16.43	324.32	400	592.17	240	644.87	19.044	17.853	18.500

Table 1: Values of the proper time regularised NJL model parameters. Tabulated are the current and constituent quark masses, infra-red and ultra-violet cut-offs, and scalar and pion effective couplings (dimensionless) evaluated at  $q^2 = m_\pi^2$  and  $q^2 = 0$ . The parameter set used  $M_\ell$ ,  $\Lambda_{\text{IR}}$ ,  $f_\pi = 93$  MeV and  $m_\pi = 140$  MeV as input to obtain remaining parameters in the usual manner.

*al.* [16] for symmetric nuclear matter and more recently by Miyatsu *et al.* [17]. We generalised the work of Krein *et al.* [16] by evaluating the full exchange terms for all octet baryons and adding them, as additional contributions, to the energy density. A consequence of this increased level of sophistication is that, if we insist on using the hyperon couplings predicted in the simple QMC model, with no meson coupling to the strange quarks, the  $\Lambda$  hyperon is no longer bound. Addressing the under-binding of the  $\Lambda$  hyperons in nuclear matter and accounting for the known existence of  $\Lambda$ -hypernuclei without the need to phenomenologically rescale couplings is a pressing issue. As the scalar couplings are dependent on the model of hadron structure through Eq. (1), it is interesting to consider an alternative to the conventionally used bag models.

The present line of research complements our recent work by changing the model for hadron structure and this, in turn, may influence nuclear matter properties and hyperon optical potentials. Throughout we use the same notation and methods as in our earlier works [12, 13, 14, 18, 19].

## 2. QMC Model for Nuclear Matter

In our calculations we consider only the spin-1/2 octet baryons. These interact via the exchange of mesons which couple directly to the quarks. The exchanged mesons included are the scalar-isoscalar ( $\sigma$ ), vector-isoscalar ( $\omega$ ), vector-isovector ( $\rho$ ) and pseudo-scalar-isovector ( $\pi$ ). These mesons only couple with the light quarks by the phenomenological OZI rule. We include the full vertex structure for the vector mesons, that is, both the Dirac and Pauli terms.

The QMC Lagrangian density used in this work is given by a combination of baryon and meson components

$$\mathcal{L} = \sum_B \mathcal{L}_B + \sum_m \mathcal{L}_m, \quad (2)$$

for the octet of baryons  $B \in \{N, \Lambda, \Sigma, \Xi\}$  and selected mesons  $m \in \{\sigma, \omega, \rho, \pi\}$  with the individual La-

grangian densities

$$\begin{aligned} \mathcal{L}_B = & \bar{\Psi}_B \left( i\gamma_\mu \partial^\mu - M_B + g_{\sigma B}(\sigma)\sigma \right. \\ & - g_{\omega B} \gamma^\mu \omega_\mu - \frac{f_{\omega B}}{2M_N} \sigma^{\mu\nu} \partial_\mu \omega_\nu \\ & - g_{\rho B} \gamma^\mu \mathbf{t} \cdot \boldsymbol{\rho}_\mu - \frac{f_{\rho B}}{2M_N} \sigma^{\mu\nu} \mathbf{t} \cdot \partial_\mu \boldsymbol{\rho}_\nu \\ & \left. - \frac{g_A}{2f_\pi} \chi_{BB} \gamma^\mu \gamma^5 \boldsymbol{\tau} \cdot \partial_\mu \boldsymbol{\pi} \right) \Psi_B, \quad (3) \end{aligned}$$

$$\begin{aligned} \sum_m \mathcal{L}_m = & \frac{1}{2} (\partial_\mu \sigma \partial^\mu \sigma - m_\sigma^2 \sigma^2) \\ & - \frac{1}{4} \boldsymbol{\Omega}_{\mu\nu} \cdot \boldsymbol{\Omega}^{\mu\nu} + \frac{1}{2} m_\omega^2 \omega_\mu \omega^\mu \\ & - \frac{1}{4} \mathbf{R}_{\mu\nu} \cdot \mathbf{R}^{\mu\nu} + \frac{1}{2} m_\rho^2 \boldsymbol{\rho}_\mu \cdot \boldsymbol{\rho}^\mu \\ & + \frac{1}{2} (\partial_\mu \boldsymbol{\pi} \cdot \partial^\mu \boldsymbol{\pi} - m_\pi^2 \boldsymbol{\pi} \cdot \boldsymbol{\pi}), \quad (4) \end{aligned}$$

for which the vector meson field strength tensors are  $\boldsymbol{\Omega}_{\mu\nu} = \partial_\mu \omega_\nu - \partial_\nu \omega_\mu$  and  $\mathbf{R}_{\mu\nu} = \partial_\mu \boldsymbol{\rho}_\nu - \partial_\nu \boldsymbol{\rho}_\mu$ .  $g_{iB}$ ,  $f_{iB}$  denote the meson-baryon coupling constants for the  $i \in \{\sigma, \omega, \rho\}$  mesons. The quantities in bold are vectors in isospin space, with isospin matrices denoted by  $\mathbf{t}$  and isospin Pauli matrices by  $\boldsymbol{\tau}$ . For nucleons and cascade particles  $\mathbf{t} = \frac{1}{2}\boldsymbol{\tau}$ . The pion-baryon interaction used here is assumed to be described by an SU(3) invariant Lagrangian with the mixing parameter  $\alpha = 2/5$  [5] from which the hyperon-pion coupling constants can be given in terms of the pion nucleon coupling [20, 5, 21].

From the Lagrangian given in Eq. (2), we use the Euler-Lagrange equations to obtain a system of coupled, non-linear partial differential equations for the quantum fields. This is a difficult system of equations to solve and to make the problem tractable a number of approximations are usually applied, including static, no sea and mean field approximations, which are implemented here. Following Refs. [22, 5, 21, 23], we decompose each meson field into two parts, a mean field part  $\langle \phi \rangle$  and a fluctuation part  $\delta\phi$ , such that  $\phi = \langle \phi \rangle + \delta\phi$ . The equations of motion are then solved order by order. The fluctuation terms are small with respect to the mean field contribution, with the exceptions being the  $\pi$  and  $\rho$  meson fluctuations.

In the Fock terms a dipole form factor is used with a cut-off  $\Lambda$ . The same cut-off is used for all mesons.

$c$ [GeV]	$G_\omega$ [GeV <sup>-2</sup> ]	$M_N$ [GeV]	$M_\Sigma$ [GeV]	$M_\Xi$ [GeV]	$M_\Lambda$ [GeV]	$g_{\sigma N}^{\text{NJL}}$	$d$ [GeV <sup>-1</sup> ]	$\omega_\Sigma$	$\omega_\Xi$	$\omega_\Lambda$	$\tilde{\omega}_\Sigma$	$\tilde{\omega}_\Xi$	$\tilde{\omega}_\Lambda$
1.141	6.279	0.94	1.23222	1.32	1.118	12.9852	1.39786	0.528979	0.38203	0.769547	0.571791	0.415508	0.752602

Table 4: Mass parametrisations for the spin-1/2 baryon octet obtained by quadratic fits to NJL model nuclear matter calculation. Tabulated quantities are the  $c$  parameter used in the static approximation, free baryon masses, the  $\sigma$ - $N$  coupling, scalar polarisability, and weights.

Model/ Scenario	$g_{\sigma N}$	$g_{\omega N}$	$g_\rho$	$K_0$ [MeV]	$L_0$ [MeV]	$U_\Lambda$ [MeV]	$U_{\Sigma^-}$ [MeV]	$U_{\Xi^-}$ [MeV]
Hartree	9.65	6.8	8.54	261	87	-55	-17	-26
Standard	8.29	8.36	4.92	263	81	-5	27	-5
$\Lambda = 1.3$	8.55	9.48	5.24	278	84	16	49	5
Dirac Only	9.41	7.95	7.66	277	82	-33	5	-19
$F_\sigma(\vec{k}) = 1$	8.86	8.11	4.24	259	75	-22	14	-14

Table 5: Couplings, nuclear matter properties, and hyperon optical potentials determined for our standard case (for which  $\Lambda = 0.9$  GeV) and variations thereof. The symmetric nuclear matter quantities evaluated at saturation,  $K_0$  and  $L_0$ , are the incompressibility and slope of the symmetry energy, respectively. The hyperon optical potentials are evaluated as in Ref. [12, 13].

$G_S$ [GeV <sup>-2</sup> ]	$G_a$ [GeV <sup>-2</sup> ]	$Z_{\{\ell\ell\}}$	$Z_{\{\ell s\}}$	$Z_{\{\ell\ell\}}$	$Z_{\{\ell s\}}$	$Z_{\{ss\}}$
7.65	2.61	14.81	16.42	3.56	3.93	4.28

Table 2: Diquark couplings determined by fitting  $M_N$  and  $g_A$ .

$M_{\{\ell\ell\}}$ [MeV]	$M_{\{\ell s\}}$ [MeV]	$M_{\{\ell\ell\}}$ [MeV]	$M_{\{\ell s\}}$ [MeV]	$M_{\{ss\}}$ [MeV]
679.18	848.71	1038.54	1170.67	1301.00

Table 3: Diquark masses determined by pole condition.

We consider several model variations, taking the cut-off  $\Lambda = 0.9$  GeV as our ‘‘Standard’’ or baseline scenario, which includes both Dirac (vector) and Pauli (tensor) interactions for the vector mesons. The other scenarios, which involve variations on the baseline are ‘‘Hartree’’, which only includes the Hartree contribution; ‘‘ $\Lambda = 1.3$  GeV’’, which has an increased cut-off; ‘‘Dirac Only’’ which neglects the tensor contribution; and finally ‘‘ $F_\sigma(\vec{k}) = 1$ ’’, where we take a hard form factor for the sigma meson, leaving the density dependence as determined within the model.

### 3. Baryon Structure in the NJL model

The NJL model [24, 25] has been extensively studied, including a large number of reviews [26, 27, 28, 29, 30, 31]. Recently various phenomena related to hadron structure have been investigated using the NJL model with Schwinger’s proper time regularisation modified in a manner that forbids the quarks to propagate on-mass-shell [32, 33], in order to simulate quark confinement [34, 19, 35, 18, 36] and dimensional reg-

ularisation [37]. In particular, the work of Ref. [19] is followed closely in the present calculation and subsequent parametrisation of the octet baryon masses.

We work with just the local (contact) four Fermi interaction between quarks, which is parametrised by a coupling constant  $G_\pi$  in the SU(3)-flavour NJL Lagrangian density. It is common to include a six-fermion term to describe phenomenologically the breaking of  $U(1)$ -axial symmetry, but as the  $\eta$  and  $\eta'$  mesons play no role in the current work, we omit this term. The dynamic breaking of chiral symmetry is evident in the spontaneous generation of constituent quark masses ( $M_u = M_d = M_\ell$  or  $M_s$ ), which are determined by the so-called gap equation [26, 27, 28, 29, 30, 31]. The application of Fierz transformations to the NJL Lagrangian rearranges the fermion fields into meson and diquark channels. The resulting diquark Lagrangian density reads [38]

$$\mathcal{L}_I^{qq} = G_S [\bar{\psi} \gamma_5 C \lambda_a \beta_A \bar{\psi}^T] [\psi^T C^{-1} \gamma_5 \lambda_a \beta_A \psi] + G_a [\bar{\psi} \gamma_\mu C \lambda_s \beta_A \bar{\psi}^T] [\psi^T C^{-1} \gamma^\mu \lambda_s \beta_A \psi], \quad (5)$$

where  $C$  corresponds to the charge conjugation matrix, which in our notation is  $C = i\gamma_2\gamma_0$ . Flavour is described by the usual SU(3) matrices  $\lambda_a$ , with ( $a = 2, 5, 7$ ), and  $\lambda_s$ , with ( $s = 0, 1, 3, 4, 6, 8$ ), while the color  $\bar{3}$  states are represented by  $\beta_A = \sqrt{3/2}\lambda_A$ , with ( $A = 2, 5, 7$ ) [38, 39, 40]. This allows the description of effective  $qq$  interactions in the scalar and axial-vector diquark channels, with strengths given by the coupling constants  $G_S$  and  $G_a$ , respectively.

Diquarks are then described as  $qq$  bound states through the solution of the Bethe-Salpeter equation depicted in Fig. 1. These solutions are given by the

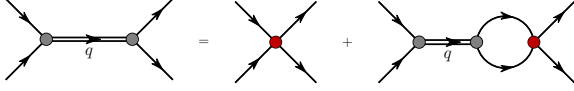


Figure 1: (Color online) Inhomogeneous Bethe-Salpeter equation for diquark correlations.

following reduced  $t$ -matrices<sup>1</sup>

$$\tau_{[q_1 q_2]}(q) = \frac{4i G_S}{1 + 2 G_S \Pi_{[q_1 q_2]}(q^2)}, \quad (6)$$

$$\tau_{[q_1 q_2]}^{\mu\nu}(q) = \frac{4i G_a}{1 + 2 G_a \Pi_{[q_1 q_2]}^T(q^2)} \left( g^{\mu\nu} - \frac{q^\mu q^\nu}{q^2} \right) + \frac{4i G_a}{1 + 2 G_a \Pi_{[q_1 q_2]}^L(q^2)} \frac{q^\mu q^\nu}{q^2}, \quad (7)$$

where the bubble diagrams read [18, 19]

$$\Pi_{[q_1 q_2]}(q^2) = 6i \int \frac{d^4 k}{(2\pi)^4} \text{Tr} \left[ \gamma_5 S_{q_1}(k) \gamma_5 S_{q_2}(k+q) \right], \quad (8)$$

$$\Pi_{[q_1 q_2]}^T(q^2) \left( g^{\mu\nu} - \frac{q^\mu q^\nu}{q^2} \right) + \Pi_{[q_1 q_2]}^L(q^2) \frac{q^\mu q^\nu}{q^2} = 6i \int \frac{d^4 k}{(2\pi)^4} \text{Tr} \left[ \gamma^\mu S_{q_1}(k) \gamma^\nu S_{q_2}(k+q) \right]. \quad (9)$$

The traces are taken over Dirac indices only and  $S_q(k)$  is the Feynman constituent quark propagator. The pole positions of the  $t$ -matrices are the masses of the different scalar and axial-vector diquarks,  $M_{[q_1 q_2]}$  and  $M_{[q_1 q_2]}^L$ , respectively. In addition, in the solution of the Faddeev equations we use the following pole approximations for the reduced  $t$ -matrices

$$\tau_{[q_1 q_2]}(q) \rightarrow \frac{-i Z_{[q_1 q_2]}}{q^2 - M_{[q_1 q_2]}^2 + i\epsilon}, \quad (10)$$

$$\tau_{[q_1 q_2]}^{\mu\nu}(q) \rightarrow \frac{-i Z_{[q_1 q_2]}}{q^2 - M_{[q_1 q_2]}^2 + i\epsilon} \left( g^{\mu\nu} - \frac{q^\mu q^\nu}{M_{[q_1 q_2]}^2} \right). \quad (11)$$

The residues at the poles define the effective couplings  $Z_{[q_1 q_2]}$  and  $Z_{[q_1 q_2]}^L$  [18, 34, 19].

For each member of the baryon octet we solve the Faddeev equations [41] in the quark-diquark picture, depicted graphically in Fig. 2. The formalism and the solution of the Faddeev equations in the present NJL model is detailed in Refs. [18, 19]. The analytic form of the homogeneous Faddeev equations is given by

$$\Gamma_B(p, s) = Z_B \Pi_B(p) \Gamma_B(p, s), \quad (12)$$

which amounts to a homogeneous Fredholm equation of the second kind for each baryon,  $B$ . Following Ishii

<sup>1</sup>We follow the notation of Refs. [18, 19] where square brackets,  $[q_1 q_2]$ , represent a scalar diquark with quark content  $q_1$  and  $q_2$ , while  $\{q_1 q_2\}$  is the corresponding axial-vector diquark.

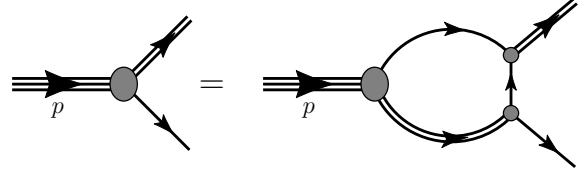


Figure 2: Homogeneous Faddeev equation for the each member of the baryon octet. The masses and vertices are found from its solution.

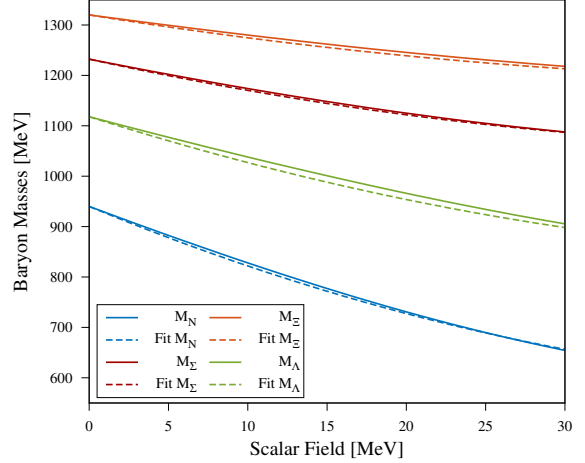


Figure 3: (Color online) Baryon octet masses vs scalar field. The data from the solution of the Faddeev equation is shown as a continuous line and the fit from Eq. (1).

*et al.* we employ the static approximation [39, 42] for the Feynman propagator of the exchanged quark. The formulation of the Faddeev kernel for each member of the octet ( $B$ ) uses the quark-diquark bubble diagrams,  $\Pi_B(p)$ , and the normalised Faddeev vertices,  $\Gamma_B(p, s)$ . The explicit form of the Faddeev vertices, bubble matrices and quark exchange kernels are explained in detail in Refs. [18, 19]. By solving the Faddeev equations we obtained the masses of the octet baryons. Note that the nucleon and cascade masses in vacuum ( $M_N$  and  $M_\Xi$ ) were used as input to constrain  $G_a$  and  $M_s$  [18, 19].

The free parameters of our model are the infra-red cut-off and the light constituent quark mass, which we take to be  $\Lambda_{IR} = 240$  MeV and  $M_\ell = 400$  MeV respectively. The infra-red cut-off is of the order of  $\Lambda_{QCD}$ , because it crudely simulates quark confinement [32, 33, 7]. For the other parameters we fit them in the following way:  $\Lambda_{UV}$  and  $G_\pi$  are fit to reproduce the experimental values of the pion's decay constant and its mass, while  $G_S$  is chosen to obtain the experimental axial charge  $g_A$  of the nucleon. The computation of  $g_A$  is done following the formalism of Ref. [18, 19].

The values of the baryon octet masses obtained are summarised in Table 4. Following the work of Bentz and Thomas [7], to account for the lack of agreement

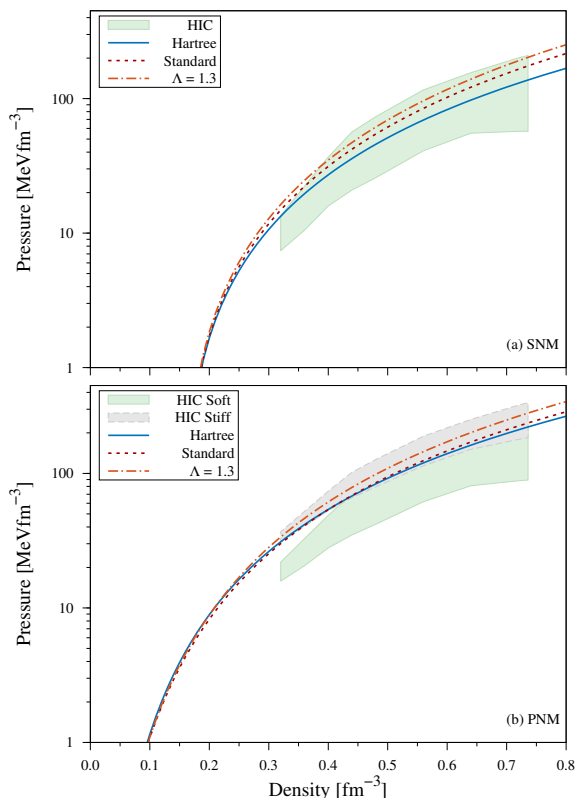


Figure 4: Pressure as a function of density in (a) SNM and (b) PNM. The constraints come from heavy-ion collision experiments deduced in Ref. [43].

between the static approximation and the exact result of the Faddeev equations in nuclear matter, the exchange quark propagator is replaced by the following interpolating function

$$\frac{1}{M_\ell^*} \rightarrow \frac{1}{M_\ell} \frac{M_\ell + c}{M_\ell^* + c}, \quad (13)$$

where  $M_\ell^*$  is the value of the constituent quark mass for a baryon in nuclear matter and  $M_\ell$  is its value inside a free baryon.  $c$  is set to 1.141 GeV and with the  $\omega N$  coupling,  $G_\omega$ , set as in Table 4, we reproduce the saturation properties of symmetric nuclear matter in the NJL model. We check that a variation of  $c$  from 0.5 GeV to 2.5 GeV makes no significant change in the results quoted here.

In the NJL model, the scalar field is related to the scalar potential  $\Phi = M_\ell^* - M_\ell$  by

$$\bar{\sigma} = \frac{\Phi}{\sqrt{Z_\pi(0)}}, \quad (14)$$

where  $Z_\pi(0)$  is defined, in analogy to Eq. (10) and (11), as the residue at the pole in the pion t-matrix. Changes in the scalar field are linked to variations of the constituent quark masses (inside the baryons and

diquarks) in nuclear matter. Consequently, the Faddeev equations were solved as a function of the in-medium constituent quark masses. The baryon masses were then parametrised as functions of mean scalar field,  $\bar{\sigma}$ , using Eq. (1) and (14). These parametrisations are given in Table 4. In Fig. 3 we show the calculated baryon masses as a function of the mean scalar field, together with the fits obtained assuming the form given by Eq. (1). The range of field strength has been chosen to correspond to the range of densities explored in Fig. 4. It is self-evident that the fits are in very good agreement with the calculated solution of the Faddeev equations.

#### 4. Nuclear Matter

We now present the numerical results for the properties of nuclear matter obtained using the self-consistent solution of the NJL model described earlier. To be definite, what we actually use from the mass parametrisations is the value of the scalar polarisability,  $d$ , and the weights,  $\omega_B$  and  $\tilde{\omega}_B$ . The vacuum contribution that would normally be included in a quark matter calculation of the EoS [12, 14] is omitted for hadronic matter.

Table 5 contains coupling constants, nuclear matter properties (incompressibility  $K_0$  and slope of the symmetry energy  $L_0$  at saturation) and hyperon optical potentials. The pressure as a function of density for SNM and PNM are shown in Fig. 4 in comparison with constraints from heavy-ion collisions. We find a slightly softer EoS when using the NJL mass parametrisations, than what we found using the bag model parametrisations in Refs. [12, 13]. This is clearly illustrated, for example, by the value of the incompressibility at saturation and in the behaviour of the pressure as a function of density, shown in Fig. 4.

The incompressibility and hyperon optical potentials show only a minor dependence on the  $c$  parameter, which was introduced to handle the quark exchange in a simplified manner. The incompressibility reduces by just 8–18 MeV when  $c$  is increased from 0.5 to 2.5 GeV. The  $\Sigma^-$  optical potential is the most sensitive of the optical potentials to a variation of  $c$ , exhibiting a reduction of 11–16 MeV, over the same range.

As the hyperon optical potentials are determined within the model without readjustment to empirically determined values, we find it encouraging to discover a reasonable level of agreement between several model variations and the empirically determined values. Of particular interest is the scenario which deviates from our standard scenario by the use of a hard scalar form factor. The motivation for taking the hard form factor only for the sigma meson is that its coupling already includes a density dependence obtained

through our model of hadron structure, which naturally acts to reduce the scalar Fock term at high density.

## 5. Summary

We have self-consistently solved for the structure of the octet baryons imbedded in nuclear matter, using the NJL model as the underlying model of hadron structure. Using those solutions we have presented numerical results for Symmetric Nuclear Matter (SNM), Pure Neutron Matter (PNM) and the hyperon optical potentials. Overall the results are very reasonable, with the properties of both SNM and PNM in good agreement with heavy ion constraints over the entire range up to five times nuclear matter density. For most of the scenarios explored the  $\Lambda$  and  $\Xi$  are bound by reasonable amounts, while the  $\Sigma$  is unbound, as suggested by phenomenological studies.

With a view to future applications to neutron star structure, we observe that the EoS is softer than what we obtained with the bag model parametrisations in our earlier work. This may well lead to a somewhat lower maximum mass, unless there is a transition to quark matter. In the near future we will explore the consequences of this model for neutron star properties, with and without such a transition. In terms of theoretical improvements it would clearly be valuable to move beyond the static approximation, making an exact solution with the full exchanged-quark propagator.

## Acknowledgements

This work was supported by the University of Adelaide and by the Australian Research Council through the ARC Centre of Excellence for Particle Physics at the Terascale CE110001004, an ARC Australian Laureate Fellowship FL0992247 and an ARC Discovery Project DP150103101.

## References

- [1] J. J. Aubert, et al., Measurement of the deuteron structure function  $F_2$  and a comparison of proton and neutron structure, *Phys. Lett.* B123 (1983) 123–126. doi:10.1016/0370-2693(83)90971-1.
- [2] D. F. Geesaman, K. Saito, A. W. Thomas, The nuclear EMC effect, *Ann. Rev. Nucl. Part. Sci.* 45 (1995) 337–390. doi:10.1146/annurev.ns.45.120195.002005.
- [3] P. A. Guichon, A Possible Quark Mechanism for the Saturation of Nuclear Matter, *Phys. Lett.* B200 (1988) 235. doi:10.1016/0370-2693(88)90762-9.
- [4] P. A. Guichon, K. Saito, E. N. Rodionov, A. W. Thomas, The Role of nucleon structure in finite nuclei, *Nucl. Phys.* A601 (1996) 349–379. arXiv:nucl-th/9509034, doi:10.1016/0375-9474(96)00033-4.
- [5] J. Rikowska-Stone, P. A. M. Guichon, H. H. Matevosyan, A. W. Thomas, Cold uniform matter and neutron stars in the quark-mesons-coupling model, *Nucl. Phys.* A792 (2007) 341–369. arXiv:nucl-th/0611030, doi:10.1016/j.nuclphysa.2007.05.011.
- [6] J. Stone, P. Guichon, P. Reinhard, A. Thomas, Finite Nuclei in the Quark-Meson Coupling Model, *Phys. Rev. Lett.* 116 (9) (2016) 092501. arXiv:1601.08131, doi:10.1103/PhysRevLett.116.092501.
- [7] W. Bentz, A. W. Thomas, The Stability of nuclear matter in the Nambu-Jona-Lasinio model, *Nucl. Phys.* A696 (2001) 138–172.
- [8] S. A. Chin, A Relativistic Many Body Theory of High Density Matter, *Annals Phys.* 108 (1977) 301–367. doi:10.1016/0003-4916(77)90016-1.
- [9] B. D. Serot, J. D. Walecka, Properties of Finite Nuclei in a Relativistic Quantum Field Theory, *Phys. Lett.* B87 (1979) 172–176. doi:10.1016/0370-2693(79)90957-2.
- [10] B. D. Serot, J. D. Walecka, The Relativistic Nuclear Many Body Problem, *Adv. Nucl. Phys.* 16 (1986) 1–327.
- [11] B. D. Serot, J. D. Walecka, Recent progress in quantum hydrodynamics, *Int. J. Mod. Phys.* E6 (1997) 515–631. arXiv:nucl-th/9701058, doi:10.1142/S0218301397000299.
- [12] D. L. Whittenbury, Hadrons and quarks in dense matter: From nuclear matter to neutron stars, Ph.D. thesis, University of Adelaide (2015).
- [13] D. L. Whittenbury, J. D. Carroll, A. W. Thomas, K. Tsushima, J. R. Stone, Quark-meson coupling model, nuclear matter constraints, and neutron star properties, *Phys. Rev. C* 89 (2014) 065801. doi:10.1103/PhysRevC.89.065801.
- [14] D. L. Whittenbury, H. H. Matevosyan, A. W. Thomas, Hybrid stars using the quark-meson coupling and proper-time Nambu-Jona-Lasinio models, *Phys. Rev.* C93 (3) (2016) 035807. arXiv:1511.08561, doi:10.1103/PhysRevC.93.035807.
- [15] P. A. M. Guichon, A. W. Thomas, K. Tsushima, Binding of hypernuclei in the latest quark-meson coupling model, *Nucl. Phys.* A814 (2008) 66–73. doi:10.1016/j.nuclphysa.2008.10.001.
- [16] G. Krein, A. W. Thomas, K. Tsushima, Fock terms in the quark meson coupling model, *Nucl. Phys.* A650 (1999) 313–325. doi:10.1016/S0375-9474(99)00117-7.
- [17] T. Miyatsu, T. Katayama, K. Saito, Effects of Fock term, tensor coupling and baryon structure variation on a neutron star, *Phys. Lett.* B709 (2012) 242–246.
- [18] M. E. Carrillo-Serrano, Properties of hadrons from a non-perturbative approach, Ph.D. thesis, University of Adelaide (2015).
- [19] M. E. Carrillo-Serrano, I. C. Cloët, A. W. Thomas,  $Su(3)$ -flavor breaking in octet baryon masses and axial couplings, *Phys. Rev. C* 90 (2014) 064316. doi:10.1103/PhysRevC.90.064316.
- [20] J. J. de Swart, The octet model and its Clebsch-Gordan coefficients, *Rev. Mod. Phys.* 35 (1963) 916–939. doi:10.1103/RevModPhys.35.916.
- [21] E. Massot, G. Chanfray, Relativistic chiral Hartree-Fock description of nuclear matter with constraints from nucleon structure and confinement, *Phys. Rev. C* 78 (2008) 015204.
- [22] P. A. M. Guichon, H. H. Matevosyan, N. Sandulescu, A. W. Thomas, Physical origin of density dependent force of the skyrme type within the quark meson coupling model, *Nucl. Phys.* A772 (2006) 1–19. doi:10.1016/j.nuclphysa.2006.04.002.
- [23] J. Hu, H. Toki, W. Wen, H. Shen, The role of the form factor and short-range correlation in the relativistic Hartree-Fock model for nuclear matter, *EPJ A* 43 (3) (2010) 323–334. doi:10.1140/epja/i2010-10917-y.
- [24] Y. Nambu, G. Jona-Lasinio, Dynamical model of elementary particles based on an analogy with superconductivity. I., *Phys.*

- Rev. 122 (1961) 345–358. doi:10.1103/PhysRev.122.345.
- [25] Y. Nambu, G. Jona-Lasinio, Dynamical model of elementary particles based on an analogy with superconductivity. II, Phys. Rev. 124 (1961) 246–254. doi:10.1103/PhysRev.124.246.
- [26] U. Vogl, W. Weise, The Nambu and Jona Lasinio model: Its implications for hadrons and nuclei, Prog. Part. Nucl. Phys. 27 (1991) 195–272. doi:10.1016/0146-6410(91)90005-9.
- [27] S. P. Klevansky, The Nambu-Jona-Lasinio model of quantum chromodynamics, Rev. Mod. Phys. 64 (1992) 649–708. doi:10.1103/RevModPhys.64.649.
- [28] T. Hatsuda, T. Kunihiro, QCD phenomenology based on a chiral effective Lagrangian, Phys. Rept. 247 (1994) 221–367. doi:10.1016/0370-1573(94)90022-1.
- [29] G. Ripka, Introduction to Nambu-Jona-Lasinio models of hadrons, Czech. J. Phys. 46 (1996) 721–750. doi:10.1007/BF01692563.
- [30] G. Ripka, Quarks bound by chiral fields: The quark-structure of the vacuum and of light mesons and baryons, Oxford Univ. Press, 1997.
- [31] M. Buballa, NJL model analysis of quark matter at large density, Phys. Rept. 407 (2005) 205–376. doi:10.1016/j.physrep.2004.11.004.
- [32] D. Ebert, T. Feldmann, H. Reinhardt, Extended NJL model for light and heavy mesons without  $q$  - anti- $q$  thresholds, Phys.Lett. B388 (1996) 154–160. arXiv:hep-ph/9608223, doi:10.1016/0370-2693(96)01158-6.
- [33] G. Hellstern, R. Alkofer, H. Reinhardt, Diquark confinement in an extended NJL model, Nucl. Phys. A625 (1997) 697–712. arXiv:hep-ph/9706551, doi:10.1016/S0375-9474(97)00412-0.
- [34] I. C. Cloet, W. Bentz, A. W. Thomas, Role of diquark correlations and the pion cloud in nucleon elastic form factors, Phys. Rev. C90 (2014) 045202. arXiv:1405.5542, doi:10.1103/PhysRevC.90.045202.
- [35] M. E. Carrillo-Serrano, W. Bentz, I. C. Cloët, A. W. Thomas,  $\rho$  meson form factors in a confining nambu-jona-lasinio model, Phys. Rev. C 92 (2015) 015212.
- [36] Y. Ninomiya, W. Bentz, I. C. Clot, Dressed Quark Mass Dependence of Pion and Kaon Form Factors, Phys. Rev. C91 (2) (2015) 025202. arXiv:1406.7212, doi:10.1103/PhysRevC.91.025202.
- [37] Z.-W. Liu, M. E. Carrillo-Serrano, A. W. Thomas, Study of Kaon Decay to Two Pions, Phys. Rev. D91 (1) (2015) 014028. arXiv:1409.2639, doi:10.1103/PhysRevD.91.014028.
- [38] N. Ishii, W. Bentz, K. Yazaki, Baryons in the NJL model as solutions of the relativistic Faddeev equation, Nucl. Phys. A587 (1995) 617–656. doi:10.1016/0375-9474(95)00032-V.
- [39] N. Ishii, W. Bentz, K. Yazaki, Faddeev approach to the nucleon in the Nambu-Jona-Lasinio (NJL) model, Phys. Lett. B301 (1993) 165–169. doi:10.1016/0370-2693(93)90683-9.
- [40] N. Ishii, W. Bentz, K. Yazaki, Solution of the relativistic three quark Faddeev equation in the Nambu-Jona-Lasinio (NJL) model, Phys. Lett. B318 (1993) 26–31. doi:10.1016/0370-2693(93)91778-L.
- [41] I. R. Afnan, A. W. Thomas, Fundamentals of Three-Body Scattering Theory, Top. Curr. Phys. 2 (1977) 1–47.
- [42] A. Buck, R. Alkofer, H. Reinhardt, Baryons as bound states of diquarks and quarks in the Nambu-Jona-Lasinio model, Phys. Lett. B286 (1992) 29–35. doi:10.1016/0370-2693(92)90154-V.
- [43] P. Danielewicz, R. Lacey, W. G. Lynch, Determination of the equation of state of dense matter, Science 298 (2002) 1592–1596. arXiv:nucl-th/0208016, doi:10.1126/science.1078070.